

Quantum critical behavior in three-dimensional one-band Hubbard model at half filling

Naoum Karchev

Department of Physics, University of Sofia, 1126 Sofia, Bulgaria

One-band Hubbard model with hopping parameter t and Coulomb repulsion U is considered at half filling. By means of the Schwinger bosons and slave Fermions representation of the electron operators and integrating out the spin-singlet Fermi fields an effective Heisenberg model with antiferromagnetic exchange constant is obtained for vectors which identifies the local orientation of the spin of the itinerant electrons. The amplitude of the spin vectors is an effective spin of the itinerant electrons accounting for the fact that some sites, in the ground state, are doubly occupied or empty. Accounting adequately for the magnon-magnon interaction the Néel temperature is calculated. When the ratio $\frac{t}{U}$ is small enough ($\frac{t}{U} \leq 0.09$) the effective model describes a system of localized electrons. Increasing the ratio increases the density of doubly occupied states which in turn decreases the effective spin and Néel temperature. The phase diagram in plane of temperature $\frac{T_N}{U}$ and parameter $\frac{t}{U}$ is presented. The quantum critical point ($T_N = 0$) is reached at $\frac{t}{U} = 0.9$. The magnons in the paramagnetic phase are studied and the contribution of the magnons' fluctuations to the heat capacity is calculated. At Néel temperature the heat capacity has a peak which is suppressed when the system approaches quantum critical point.

PACS numbers: 64.70.Tg, 71.10.Fd, 75.50.Ee, 75.40.Cx

I. INTRODUCTION

Quantum phase transitions arise in many-body systems because of competing interactions that support different ground states. At quantum critical point (QCP) the matter undergoes a transition from one phase to another at zero temperature. A nonthermal control parameter, such as pressure, drives the system to QCP. The typical temperature-pressure phase diagrams observed in the heavy-fermion materials $CePd_2Si_2$, $CeIn_3$, $CeRh_2Si_2$, $CeCu_2Si_2$ and $CeRhIn_5$ [1–6] show that at ambient pressure the compounds order into antiferromagnets below the Néel temperature T_N . Applying pressure reduces T_N monotonically. The QCP is the critical pressure at which the Néel temperature $T_N = 0$.

The quantum critical behavior has been extensively studied for many years. Many books [7, 8], review articles [9–15] and papers investigate systematically the magnetic quantum critical point.

The magnetism of cerium based compounds is determined by the $4f$ electrons of Ce^{3+} ions. The strong spin-orbit coupling splits the $4f$ electrons into $j = \frac{5}{2}$ and $j = \frac{7}{2}$ multiplets, where j is the total angular momentum. Only the sextuplet effectively contributes to the low energy excitations. It is further split into Γ_7 doublet and Γ_8 quadruplet due to crystal electric field. For isotropic systems like $CeIn_3$, the energy level of Γ_7 is lowest. The eigenstates are $|\Gamma_{7\pm}\rangle = \sqrt{\frac{1}{6}}|\pm\frac{5}{2}\rangle - \sqrt{\frac{5}{6}}|\mp\frac{3}{2}\rangle$, where " + " and " - " denote up and down "pseudo-spins" respectively. The three-dimensional (3D) one-band Hubbard model is the simplest model of itinerant magnetism of the isotropic cerium based compounds. Although the hybridization with $In5p$ electronic states may be important, here it is considered as a renormalization of the hopping amplitude.

The ground state of the 3D Hubbard model on a simple cubic lattice, at half filling has antiferromagnetic long range order for all positive values of the onsite Coulomb repulsion. There have been many attempts to calculate Néel temperature T_N using quantum Monte Carlo (QMC) simulations [16–19], variational methods [20, 21], Hartree Fock theory [22], strong coupling expansions [24], and dynamical mean field theory (DMFT) [25–27]. Calculations beyond the dynamical mean field theory: the dynamical cluster approximation (DCA) [28], cluster generalization of the DMFT [29] and dynamical vertex approximation (DGA) [30, 31] have been proposed. All these studies do not show any trace of quantum critical point.

Here we focus attention on the quantum critical behavior in itinerant antiferromagnets. The increasing of the double occupancy in 3D one-band Hubbard model at half filling pushes the system to the quantum criticality. Increasing the ratio $\frac{t}{U}$, where t is the hopping parameter and U is the Coulomb repulsion, increases the density of doubly occupied states which in turn decreases the effective spin and Néel temperature. The Quantum Critical Point is a state with a critically high density of the doubly occupied state.

The physics of the antiferromagnets near the Néel temperature is dominated by the magnons' fluctuations and it is important to account for them in the best way. We employ a technique of calculation, which captures the essentials of the magnons' fluctuations in the theory, and for 2D systems one obtains zero Néel temperature, in accordance with Mermin-Wagner theorem [33].

The paper is organized as follows. In Sec. II, starting from one-band Hubbard model at half filling, with hopping parameter t and Coulomb repulsion U , we derive an effective Heisenberg-like model, with antiferromagnetic exchange constant, in terms of the vector describing the local orientations of the magnetization. The transversal

fluctuations of the vector are the magnons in the theory. The amplitude m of the spin vectors is an effective spin of the itinerant electrons accounting for the fact that some sites, in the ground state, are doubly occupied or empty. This is a base for Néel temperature calculation. Section III is devoted to $T_N/J - m$ and $T_N/U - t/U$ phase diagrams of the model. The paramagnetic phase of itinerant antiferromagnets is explored in Section IV. The calculations of the specific heat for different values of the control parameter t/U are presented in the Section V. A summary in Sec. VI concludes the paper.

II. EFFECTIVE MODEL

We consider a theory with Hamiltonian

$$h = -t \sum_{\langle ij \rangle} (c_{i\sigma}^\dagger c_{j\sigma} + h.c.) + U \sum_i n_{i\uparrow} n_{i\downarrow} - \mu \sum_i n_i \quad (1)$$

where $c_{i\sigma}^\dagger$ and $c_{i\sigma}$ ($\sigma = \uparrow, \downarrow$) are creation and annihilation operators for spin-1/2 Fermi operators of itinerant electrons, $n_{i\sigma} = c_{i\sigma}^\dagger c_{i\sigma}$, $n_i = n_{i\uparrow} + n_{i\downarrow}$, $t > 0$ is the hopping parameter, $U > 0$ is the the Coulomb repulsion and μ is the chemical potential. The sums are over all sites of a three-dimensional cubic lattice, and $\langle i, j \rangle$ denotes the sum over the nearest neighbors.

We represent the Fermi operators, the spin of the itinerant electrons

$$s_i^\nu = \frac{1}{2} \sum_{\sigma\sigma'} c_{i\sigma}^\dagger \tau_{\sigma\sigma'}^\nu c_{i\sigma'}, \quad (2)$$

where (τ^x, τ^y, τ^z) are Pauli matrices, and the density operators $n_{i\sigma}$ in terms of the Schwinger bosons $(\varphi_{i,\sigma}, \varphi_{i,\sigma}^\dagger)$ and slave Fermions $(h_i, h_i^\dagger, d_i, d_i^\dagger)$. The Bose fields are doublets ($\sigma = 1, 2$) without charge, while Fermions are spinless with charges 1 (d_i) and -1 (h_i).

$$\begin{aligned} c_{i\uparrow} &= h_i^\dagger \varphi_{i1} + \varphi_{i2}^\dagger d_i, & c_{i\downarrow} &= h_i^\dagger \varphi_{i2} - \varphi_{i1}^\dagger d_i, \\ n_i &= 1 - h_i^\dagger h_i + d_i^\dagger d_i, & s_i^\nu &= \frac{1}{2} \sum_{\sigma\sigma'} \varphi_{i\sigma}^\dagger \tau_{\sigma\sigma'}^\nu \varphi_{i\sigma'}, \\ c_{i\uparrow}^\dagger c_{i\uparrow} c_{i\downarrow}^\dagger c_{i\downarrow} &= d_i^\dagger d_i \end{aligned} \quad (3)$$

$$\varphi_{i1}^\dagger \varphi_{i1} + \varphi_{i2}^\dagger \varphi_{i2} + d_i^\dagger d_i + h_i^\dagger h_i = 1 \quad (4)$$

To solve the constraint (Eq.4), one makes a change of variables, introducing Bose doublets $\zeta_{i\sigma}$ and $\zeta_{i\sigma}^\dagger$ [34]

$$\begin{aligned} \zeta_{i\sigma} &= \varphi_{i\sigma} (1 - h_i^\dagger h_i - d_i^\dagger d_i)^{-\frac{1}{2}}, \\ \zeta_{i\sigma}^\dagger &= \varphi_{i\sigma}^\dagger (1 - h_i^\dagger h_i - d_i^\dagger d_i)^{-\frac{1}{2}}, \end{aligned} \quad (5)$$

where the new fields satisfy the constraint $\zeta_{i\sigma}^\dagger \zeta_{i\sigma} = 1$. In terms of the new fields the spin vectors of the itinerant electrons Eq.(2) have the form

$$s_i^\nu = \frac{1}{2} \sum_{\sigma\sigma'} \zeta_{i\sigma}^\dagger \tau_{\sigma\sigma'}^\nu \zeta_{i\sigma'} [1 - h_i^\dagger h_i - d_i^\dagger d_i] \quad (6)$$

When, in the ground state, the lattice site is empty, the operator identity $h_i^\dagger h_i = 1$ is true. When the lattice site is doubly occupied, $d_i^\dagger d_i = 1$. Hence, when the lattice site is empty or doubly occupied the spin on this site is zero. When the lattice site is neither empty nor doubly occupied ($h_i^\dagger h_i = d_i^\dagger d_i = 0$), the spin equals $\mathbf{s}_i = 1/2 \mathbf{n}_i$, where the unit vector

$$n_i^\nu = \sum_{\sigma\sigma'} \zeta_{i\sigma}^\dagger \tau_{\sigma\sigma'}^\nu \zeta_{i\sigma'} \quad (\mathbf{n}_i^2 = 1) \quad (7)$$

identifies the local orientation of the spin of the itinerant electron.

The Hamiltonian Eq.(1), rewritten in terms of Bose fields Eq.(5) and slave Fermions, adopts the form

$$\begin{aligned} h &= -t \sum_{\langle ij \rangle} [(d_j^\dagger d_i - h_j^\dagger h_i) \zeta_{i\sigma}^\dagger \zeta_{j\sigma} \\ &+ (d_j^\dagger h_i^\dagger - d_i^\dagger h_j^\dagger) (\zeta_{i1} \zeta_{j2} - \zeta_{i2} \zeta_{j1}) + h.c.] \\ &\times (1 - h_i^\dagger h_i - d_i^\dagger d_i)^{\frac{1}{2}} (1 - h_j^\dagger h_j - d_j^\dagger d_j)^{\frac{1}{2}} \\ &+ U \sum_i d_i^\dagger d_i - \mu \sum_i (1 - h_i^\dagger h_i + d_i^\dagger d_i), \end{aligned} \quad (8)$$

An important advantage of working with Schwinger bosons and slave Fermions is the fact that Hubbard term is in a diagonal form. The fermion-fermion and fermion-boson interactions are included in the hopping term. One treats them as a perturbation. To proceed we approximate the hopping term of the Hamiltonian Eq.(8) setting $(1 - h_i^\dagger h_i - d_i^\dagger d_i)^{\frac{1}{2}} \sim 1$ and keep only the quadratic, with respect to Fermions, terms. This means that the averaging in the subspace of the Fermions is performed in one fermion-loop approximation. Further, we represent the resulting Hamiltonian as a sum of two terms

$$h = h_0 + h_{int}, \quad (9)$$

where

$$\begin{aligned} h_0 &= -t \sum_{\langle ij \rangle} (d_j^\dagger d_i - h_j^\dagger h_i + h.c.) + U \sum_i d_i^\dagger d_i \\ &- \mu \sum_i (1 - h_i^\dagger h_i + d_i^\dagger d_i), \end{aligned} \quad (10)$$

is the Hamiltonian of the free d and h fermions, and

$$\begin{aligned} h_{int} &= -t \sum_{\langle ij \rangle} [(d_j^\dagger d_i - h_j^\dagger h_i) (\zeta_{i\sigma}^\dagger \zeta_{j\sigma} - 1) \\ &+ (d_j^\dagger h_i^\dagger - d_i^\dagger h_j^\dagger) (\zeta_{i1} \zeta_{j2} - \zeta_{i2} \zeta_{j1}) + h.c.] \end{aligned} \quad (11)$$

is the Hamiltonian of boson-fermion interaction.

The ground state of the system, without accounting for the spin fluctuations, is determined by the free-fermion Hamiltonian h_0 and is labeled by the density of electrons

$$n = 1 - \langle h_i^\dagger h_i \rangle + \langle d_i^\dagger d_i \rangle \quad (12)$$

(see equation (3)) and the "effective spin" of the electron

$$m = \frac{1}{2} (1 - \langle h_i^+ h_i \rangle - \langle d_i^+ d_i \rangle). \quad (13)$$

At half filling

$$\langle h_i^+ h_i \rangle = \langle d_i^+ d_i \rangle. \quad (14)$$

To solve this equation, for all values of the parameters U and t , one sets the chemical potential $\mu = U/2$. Utilizing this representation of μ we calculate the effective spin "m" as a function of the ration t/U . The result is depicted in figure (1).

Let us introduce the vector,

$$M_i^\nu = m \sum_{\sigma\sigma'} \zeta_{i\sigma}^+ \tau_{\sigma\sigma'}^\nu \zeta_{i\sigma'} \quad \mathbf{M}_i^2 = m^2. \quad (15)$$

Then, the spin-vector of itinerant electrons Eq.(6) can be written in the form

$$\mathbf{s}_i = \frac{1}{2m} \mathbf{M}_i (1 - h_i^+ h_i - d_i^+ d_i), \quad (16)$$

where the vector \mathbf{M}_i identifies the local orientation of the spin of the itinerant electrons. The contribution of itinerant electrons to the total magnetization is $\langle \mathbf{s}_i^z \rangle$. Accounting for the definition of m (see Eq.13), one obtains $\langle \mathbf{s}_i^z \rangle = \langle \mathbf{M}_i^z \rangle$.

The Hamiltonian is quadratic with respect to the Fermions d_i, d_i^+ and h_i, h_i^+ , and one can average in the subspace of these Fermions (to integrate them out in the path integral approach). As a result, one obtains an effective model for vectors \mathbf{M}_i , which identifies the local orientation of the spin of the itinerant electrons, with Hamiltonian

$$h_{eff} = J \sum_{\langle ij \rangle} \mathbf{M}_i \cdot \mathbf{M}_j \quad (17)$$

The effective exchange constant J is calculated in the one loop approximation and in the limit when the frequency and the wave vector are small. At zero temperature, one obtains

$$J = -\frac{t}{6m^2} \frac{1}{N} \sum_k \left(\sum_{\nu=1}^3 \cos k_\nu \right) [\theta(-\varepsilon_k^d) + \theta(-\varepsilon_k^h)] + \frac{2t^2}{3m^2U} \frac{1}{N} \sum_k \left(\sum_{\nu=1}^3 \sin^2 k_\nu \right) [1 - \theta(-\varepsilon_k^h) - \theta(-\varepsilon_k^d)] \quad (18)$$

where N is the number of lattice's sites, ε_k^h and ε_k^d are Fermions' dispersions,

$$\begin{aligned} \varepsilon_k^h &= 2t(\cos k_x + \cos k_y + \cos k_z) + \mu \\ \varepsilon_k^d &= -2t(\cos k_x + \cos k_y + \cos k_z) + U - \mu, \end{aligned} \quad (19)$$

and the wave vector k runs over the first Brillouin zone of a cubic lattice.

The exchange constant J and the effective spin m are function of the ratio t/U . At half filling the exchange constant J is positive and the model (17) is an effective model of itinerant antiferromagnetism. The functions $m(t/U)$ and $J(t/U)/U$ are depicted in figure (1). At half filling the density of doubly occupied states $\langle d^+ d \rangle$ is equal to the density of empty states $\langle h^+ h \rangle$. Increasing the ratio t/U increases the density of doubly occupied states which in turn decreases the effective spin of the system (see equation (13)).

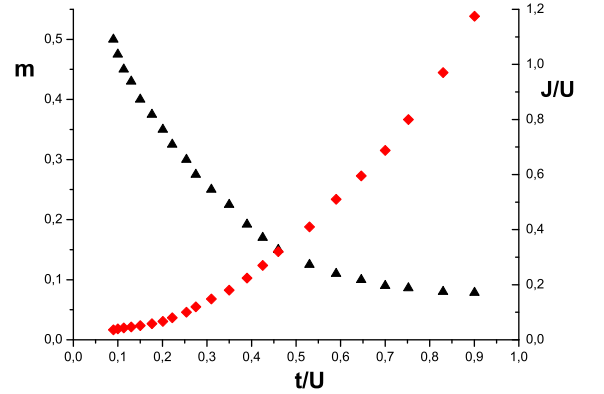


FIG. 1: (Color online) The effective spin of the system m as a function of the ratio t/U -black triangles(left scale). Dimensionless exchange constant J/U as a function of t/U -red rhombuses(right scale).

III. PHASE DIAGRAM

We are going to study the antiferromagnetic phase of the model Eq.(17) with $J > 0$. To proceed, one uses the Holstein-Primakoff representation of the spin vectors $\mathbf{M}_j(a_j^+, a_j)$, where a_j^+, a_j are Bose fields.

$$\begin{aligned} M_j^+ &= M_j^1 + iM_j^2 \\ &= \cos^2 \frac{\theta_j}{2} \sqrt{2m - a_j^+ a_j} a_j - \sin^2 \frac{\theta_j}{2} a_j^+ \sqrt{2m - a_j^+ a_j} \\ M_j^- &= M_j^1 - iM_j^2 \\ &= \cos^2 \frac{\theta_j}{2} a_j^+ \sqrt{2m - a_j^+ a_j} - \sin^2 \frac{\theta_j}{2} \sqrt{2m - a_j^+ a_j} a_j \\ M_j^3 &= \cos \theta_j (m - a_j^+ a_j) \end{aligned} \quad (20)$$

where $\theta_j = \mathbf{Q} \cdot \mathbf{r}_j$ and $\mathbf{Q} = (\pi, \pi, \pi)$ is the antiferromagnetic wave vector. In terms of the Bose fields and keeping only the quadratic and quartic terms, the effective Hamiltonian (Eq.17) adopts the form

$$h_{eff} = h_2 + h_4 \quad (21)$$

where

$$h_2 = Jm \sum_{\langle ij \rangle} (a_i^+ a_i + a_j^+ a_j - a_i^+ a_j^+ - a_i a_j) \quad (22)$$

$$h_4 = \frac{J}{4} \sum_{\langle ij \rangle} (a_i^+ a_j^+ a_j^+ a_j + a_i^+ a_i^+ a_j^+ a_i + a_i^+ a_i a_i a_j + a_j^+ a_j a_j a_i - 4a_i^+ a_j^+ a_i a_j) \quad (23)$$

and the terms without Bose fields are dropped.

The next step is to represent the Hamiltonian in the Hartree-Fock approximation. To this end one represents the product of two Bose fields in the form

$$a_i^+ a_j = a_i^+ a_j - \langle a_i^+ a_j \rangle + \langle a_i^+ a_j \rangle \quad (24)$$

and neglects all terms $(a_i^+ a_j - \langle a_i^+ a_j \rangle)^2$ in the four magnon interaction Hamiltonian. The result is

$$\begin{aligned} a_i^+ a_j^+ a_j^+ a_j &\approx -\langle a_i^+ a_j^+ \rangle \langle a_j^+ a_j \rangle \\ &\quad + a_i^+ a_j^+ \langle a_j^+ a_j \rangle + a_j^+ a_j \langle a_i^+ a_j^+ \rangle \\ a_i^+ a_i^+ a_j^+ a_i &\approx -\langle a_i^+ a_i \rangle \langle a_i^+ a_j^+ \rangle \\ &\quad + a_i^+ a_j^+ \langle a_i^+ a_i \rangle + a_i^+ a_i \langle a_i^+ a_j^+ \rangle \\ a_i^+ a_i a_i a_j &\approx -\langle a_i^+ a_i \rangle \langle a_i a_j \rangle \\ &\quad + a_i a_j \langle a_i^+ a_i \rangle + a_i^+ a_i \langle a_i a_j \rangle \\ a_j^+ a_j a_j a_i &\approx -\langle a_j^+ a_j \rangle \langle a_j a_i \rangle \\ &\quad + a_j a_i \langle a_j^+ a_j \rangle + a_j^+ a_j \langle a_j a_i \rangle \\ 2a_i^+ a_j^+ a_i a_j &\approx -\langle a_i^+ a_j^+ \rangle \langle a_i a_j \rangle \\ &\quad - \langle a_i^+ a_i \rangle \langle a_j^+ a_j \rangle \\ &\quad + a_i^+ a_j^+ \langle a_i a_j \rangle + a_i a_j \langle a_i^+ a_j^+ \rangle \\ &\quad + a_i^+ a_i \langle a_j^+ a_j \rangle + a_j^+ a_j \langle a_i^+ a_i \rangle \end{aligned} \quad (25)$$

We assume that the matrix elements do not depend on the lattice's links and $\langle a_i^+ a_j^+ \rangle = \langle a_i a_j \rangle$. Then the Hartree-Fock approximation for the effective Hamiltonian (Eq.21) can be represented as a sum

$$h_{eff} \approx h_{HF} = h_{cl} + h_q \quad (26)$$

where

$$h_{cl} = 6Jm^2 N(r-1)^2, \quad (27)$$

$$h_q = Jmr \sum_{\langle ij \rangle} (a_i^+ a_i + a_j^+ a_j - a_i^+ a_j^+ - a_i a_j) \quad (28)$$

and r is the Hartree-Fock parameter, to be determined self-consistently from the equation

$$\begin{aligned} r &= 1 - \frac{1}{2m} \frac{1}{N} \sum_k \langle a_k^+ a_k \rangle \\ &\quad + \frac{1}{2m} \frac{1}{N} \sum_k \frac{\cos k_x + \cos k_y + \cos k_z}{3} \langle a_k^+ a_{-k}^+ \rangle. \end{aligned} \quad (29)$$

Equation (28) shows that the Hartree-Fock parameter r renormalizes the exchange constant J .

It is convenient to rewrite the Hamiltonian (Eq.28) in momentum space representation:

$$h_q = \sum_k [\varepsilon a_k^+ a_k - \gamma_k (a_k^+ a_{-k}^+ + a_k a_{-k})] \quad (30)$$

where

$$\varepsilon = 6Jmr \quad (31)$$

$$\gamma_k = Jmr (\cos k_x + \cos k_y + \cos k_z)$$

To diagonalize the Hamiltonian one introduces new Bose field α_k , α_k^+ by means of the transformation

$$a_k = u_k \alpha_k + v_k \alpha_{-k}^+ \quad a_k^+ = u_k \alpha_k^+ + v_k \alpha_{-k} \quad (32)$$

where the coefficients of the transformation u_k and v_k are real functions of the wave vector k

$$\begin{aligned} u_k &= \sqrt{\frac{1}{2} \left(\frac{\varepsilon}{\sqrt{\varepsilon^2 - 4\gamma_k^2}} + 1 \right)} \\ v_k &= \text{sign}(\gamma_k) \sqrt{\frac{1}{2} \left(\frac{\varepsilon}{\sqrt{\varepsilon^2 - 4\gamma_k^2}} - 1 \right)} \end{aligned} \quad (33)$$

The transformed Hamiltonian adopts the form

$$h_q = \sum_{k \in B_r} (E_k \alpha_k^+ \alpha_k + E_k^0), \quad (34)$$

with dispersion

$$E_k = \sqrt{\varepsilon^2 - 4\gamma_k^2} \quad (35)$$

and vacuum energy

$$E_k^0 = \frac{1}{2} \left[\sqrt{\varepsilon^2 - 4\gamma_k^2} - \varepsilon \right] \quad (36)$$

For positive values of the Hartree-Fock parameter and all values of $k \in B$, the dispersion is nonnegative $E_k \geq 0$. It is equal to zero at $\mathbf{k} = (0, 0, 0)$ and $\mathbf{k}^* = (\pm\pi, \pm\pi, \pm\pi)$. Therefor, α_k -Boson describes the two long-range excitations (magnons) in the spin system [35]. Near these vectors the dispersion adopts the form $E_k \propto c_s |\mathbf{k}|$ and $E_k \propto c_s |\mathbf{k} - \mathbf{k}^*|$ with spin-wave velocity $c_s = 2\sqrt{3}Jmr$.

One can rewrite the equation for the Hartree-Fock parameter (Eq.29) in terms of the α_k field

$$\begin{aligned} r(T) &= 1 + \frac{1}{4m} - \frac{1}{12m} \frac{1}{N} \sum_k \sqrt{9 - e_k^2} [1 + 2n_k(T)] \\ e_k &= \cos k_x + \cos k_y + \cos k_z \end{aligned} \quad (37)$$

where n_k is the Bose function of the α excitations

$$n_k(T) = \frac{1}{e^{\frac{E_k}{T}} - 1}. \quad (38)$$

It is important to stress that the equation (37) can be obtained from the equation

$$\partial \mathcal{F} / \partial r = 0 \quad (39)$$

where \mathcal{F} is the free energy of a system with Hamiltonian h_{HF} (Eq.26)

$$\mathcal{F} = 6Jm^2(r-1)^2 + \frac{1}{N} \sum_k E_k^0 + \frac{T}{N} \sum_k \ln \left(1 - e^{-\frac{E_k}{T}} \right). \quad (40)$$

The sublattice magnetizations M^A and M^B for sublattice A ($\cos \theta_i = 1$) and sublattice B ($\cos \theta_i = -1$) are defined by the equation (20). It is evident that $M^A = -M^B$, so that the total magnetization is zero. In terms of the Bose function n_k of the α excitations they adopt the form

$$\begin{aligned} M^A(T) &= -M^B(T) = m - \frac{1}{N} \sum_k \langle a_k^+ a_k \rangle \quad (41) \\ &= m + \frac{1}{2} - \frac{1}{2N} \sum_k \frac{3}{\sqrt{9 - e_k^2}} [1 + 2n_k(T)] \end{aligned}$$

At Néel temperature T_N the sublattice magnetization is zero $M^A(T_N) = -M^B(T_N) = 0$. From equation (41) and equation (37) rewritten at Néel temperature one obtains a system of equations which determines the Néel temperature

$$\begin{aligned} r(T_N) &= 1 + \frac{1}{4m} - \frac{1}{12m} \frac{1}{N} \sum_k \sqrt{9 - e_k^2} [1 + 2n_k(T_N)] \\ 2m + 1 &= \frac{1}{N} \sum_k \frac{3}{\sqrt{9 - e_k^2}} [1 + 2n_k(T_N)] \quad (42) \end{aligned}$$

To clarify the importance of the notion effective spin m one investigates the relationship between Néel temperature and m . The dependence of the dimensionless temperature T_N/J on effective spin is depicted in figure (2). Decreasing the effective spin decreases the Néel temperature. The quantum critical value of the effective spin, the value at which $T_N = 0$, is $m_{cr} = 0.078$. The effective spin decreases because the density of the doubly occupied states increases. The quantum critical point is a state with domination of the doubly occupied sites.

Utilizing the dependence of the effective spin m and the exchange constant J/U on the parameter t/U (see figure 1) one can obtain the dependence of the dimensionless temperature T_N/U on the ratio t/U . The phase diagram in plane of temperature T_N/U and control parameter t/U is depicted in figure (3). The quantum critical value of the ratio is $t/U = 0.9$.

To compare with experimental temperature-pressure curves one have to establish the relationship between hopping parameter t and pressure and between Coulomb repulsion U and pressure. The simplest assumption that U is a constant and t is a linear function of the pressure leads to a result which well reproduces the temperature-pressure phase diagram of $CeRhIn_5$. But, to obtain the

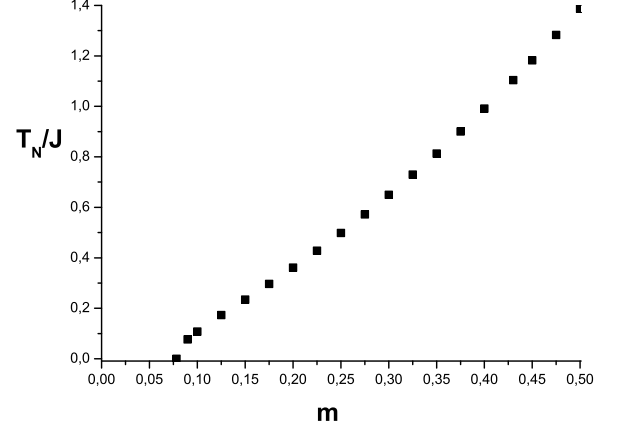


FIG. 2: (Color online) The dependence of the dimensionless temperature T_N/J on the effective spin of the itinerant electron m . The quantum critical value of the effective spin, the value at which $T_N = 0$, is $m_{cr} = 0.078$

experimental phase diagrams of $CePd_2Si_2$ or $CeIn_3$ one has to implement much more complicate fitting procedure.

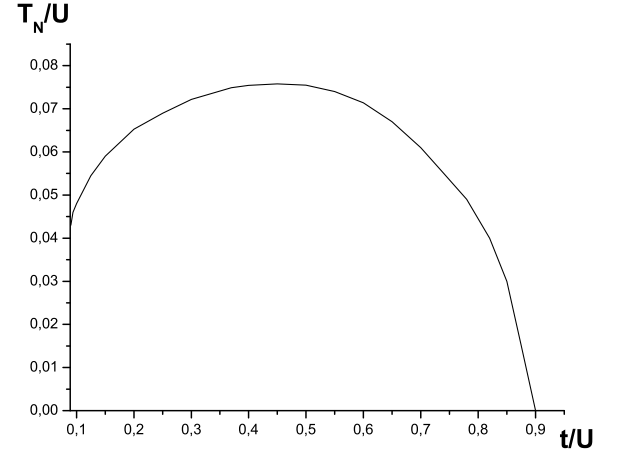


FIG. 3: (Color online) Phase diagram in plane of temperature T_N/U and control parameter t/U . The quantum critical value of the ratio is $t/U = 0.9$

IV. PARAMAGNETIC PHASE

When the system undergoes thermal ($T_N > 0$) or quantum ($T_N = 0$) transition to paramagnetic state, the magnon's dispersion opens a gap. This is a generic feature of the second order phase transition. To describe it mathematically, one utilizes the modified spin-wave the-

ory proposed to describe 2D ferromagnetic [36, 37] and antiferromagnetic [38, 39] systems at finite temperature. The Takahashi's idea is to supplement the spin-wave theory with the constraint that the magnetization be zero. In the present paper we formulate, along the same line, a modified spin-wave theory of the paramagnetic phase.

To enforce the magnetization on the two sublattices to be equal to zero in paramagnetic phase, one introduces parameter λ , and the new Hamiltonian is obtained from the old one (Eq. 17) by adding a new term

$$\hat{h} = h_{eff} - \lambda \sum_i (m - a_i^+ a_i) \quad (43)$$

This modification leads to a modification of the Hamiltonian (Eq.30). One obtains

$$\hat{h}_q = \sum_k [\hat{\varepsilon} a_k^+ a_k - \gamma_k (a_k^+ a_{-k}^+ + a_k a_{-k})] \quad (44)$$

with

$$\hat{\varepsilon} = 6Jmr + \lambda \quad (45)$$

We implement the same calculations as above and arrive at a Hamiltonian which is modification of the Hamiltonian (Eq.34)

$$\hat{h}_q = \sum_{k \in B} (\hat{E}_k \alpha_k^+ \alpha_k + \hat{E}_k^0), \quad (46)$$

with new dispersion

$$\hat{E}_k = \sqrt{\hat{\varepsilon}^2 - 4\gamma_k^2} \quad (47)$$

and new vacuum energy

$$\hat{E}_k^0 = \frac{1}{2} \left[\sqrt{\hat{\varepsilon}^2 - 4\gamma_k^2} - \hat{\varepsilon} \right] \quad (48)$$

The free energy $\hat{\mathcal{F}}$ of a system with the modified Hamiltonian reads

$$\hat{\mathcal{F}} = 6Jm^2(r-1)^2 + \frac{1}{N} \sum_k \hat{E}_k^0 + \frac{T}{N} \sum_k \ln \left(1 - e^{-\frac{\hat{E}_k}{T}} \right). \quad (49)$$

Then, one can obtain the system of equations for the Hartree-Fock parameter and the parameter λ from the equations

$$\partial \mathcal{F} / \partial r = 0, \quad \partial \mathcal{F} / \partial \lambda = 0. \quad (50)$$

The result is

$$\begin{aligned} r(T) &= 1 + \frac{1}{4m} \\ &- \frac{1}{12m} \frac{1}{N} \sum_k \frac{3\hat{\varepsilon} - 2Jmr\epsilon_k^2}{\sqrt{\hat{\varepsilon}^2 - 4\gamma_k^2}} [1 + 2\hat{n}_k(T)] \\ 2m + 1 &= \frac{1}{N} \sum_k \frac{\hat{\varepsilon}}{\sqrt{\hat{\varepsilon}^2 - 4\gamma_k^2}} [1 + 2\hat{n}_k(T)] \end{aligned} \quad (51)$$

where \hat{n}_k is the Bose function of α excitation (Eq.38) with new dispersion \hat{E}_k (Eq.47).

It is convenient to represent the parameter λ in the form

$$\lambda = 6Jm\kappa \quad (52)$$

introducing a new parameter κ . Near to the zero wave vector the dispersion adopts the form $\hat{E}_k \propto \sqrt{c_s^2 |\mathbf{k}|^2 + 36Jmr(2\kappa + \kappa^2)}$, where $36Jmr(2\kappa + \kappa^2)$ is the gap of the magnon. It is zero below Néel temperature and increases when the temperature increases above Néel temperature.

We implement the following procedure to calculate the Hartree-Fock parameter r and the parameter κ . At temperatures below the Néel temperature $\kappa = 0$ and $r(T/J)$ is obtained from equation (37). At temperatures above the Néel temperature the functions $r(T/J)$ and $\kappa(T/J)$ are solution of the system (51). The result is depicted in figures (4) and (5).

The figure (4) shows that the renormalization r at zero temperature, due to the magnon-magnon interaction, is stronger when the system approaches quantum critical point (curve "a"), and it is insignificant for spin-localized systems (curve "d").

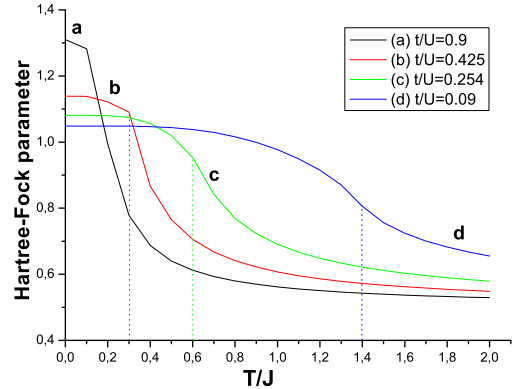


FIG. 4: (Color online) The dependence of the Hartree-Fock parameter on the dimensionless temperature T/J : (a) at quantum critical point $t/U = 0.9$ ($m_{cr} = 0.078$); (b) at $t/U = 0.425$ ($m = 0.175$); (c) at $t/U = 0.254$ ($m = 0.3$); (d) at $t/U = 0.09$ ($m = 0.5$). The vertical dot lines correspond to the Néel temperatures T_N/J .

The κ parameter is a measure for the gap of the magnon in paramagnetic phase. It is zero at Néel temperature and increases when the temperature increases. The function $\kappa(T/J)$ is depicted in figure (5) for different values of the ratio t/U .

The figure (5) shows that the increase is faster when the system approaches quantum critical point (curve "a"), and it is weak for spin-localized systems (curve "d").

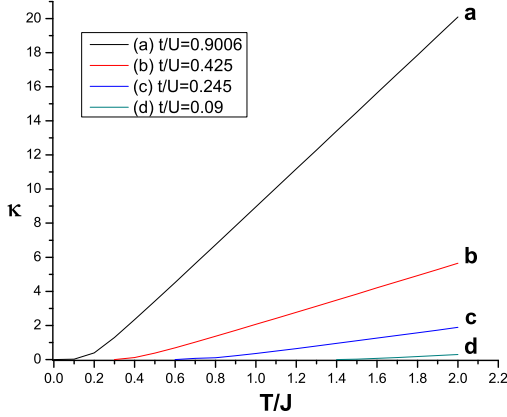


FIG. 5: (Color online) The dependence of κ parameter on the dimensionless temperature T/J : (a) at quantum critical point $t/U = 0.9$; (b) at $t/U = 0.425$; (c) at $t/U = 0.254$; (d) at $t/U = 0.09$.

V. SPECIFIC HEAT

Utilizing the above calculated functions $r(T/J)$ and $\kappa(T/J)$ one can calculate the magnons' contribution to the specific heat of the system. By definition, the entropy is

$$S = -\frac{dF}{dT} = -\frac{\partial F}{\partial r} \frac{\partial r}{\partial T} - \frac{\partial F}{\partial \lambda} \frac{\partial \lambda}{\partial T} - \frac{\partial F}{\partial T} \quad (53)$$

where F is the free energy of the system Eqs.(40,49). Owing to the equations (39) and (50) the first two terms in Eq.(53) are equal to zero and one obtains the customary formula for the entropy of a Bose system

$$S = \frac{1}{N} \sum_k [(1 + n_k) \ln(1 + n_k) - n_k \ln n_k], \quad (54)$$

where the dispersion E_k Eq.(35) is used to define the Bose function Eq.(38) below the Néel temperature, and dispersion \hat{E}_k Eq.(47) above it. With entropy, as a function of temperature in mind, one can calculate the contribution of magnons to the specific heat.

$$C_v = T \frac{dS}{dT} \quad (55)$$

The resultant curves $C_v(T/J)$, for different values of the parameter t/U , are depicted in figure (6).

The function $C_v(T/J)$ has a maximum at Néel temperature. The figure (6) shows that the maximum is suppressed at quantum critical point (curve "a"). The maximum is well observed experimentally[32, 40], and one can use it to determine the Néel temperature. The experimental measurements of the specific heat of $CeRhIn_5$ for different pressures [32] show that at T_N , C_v/T has a

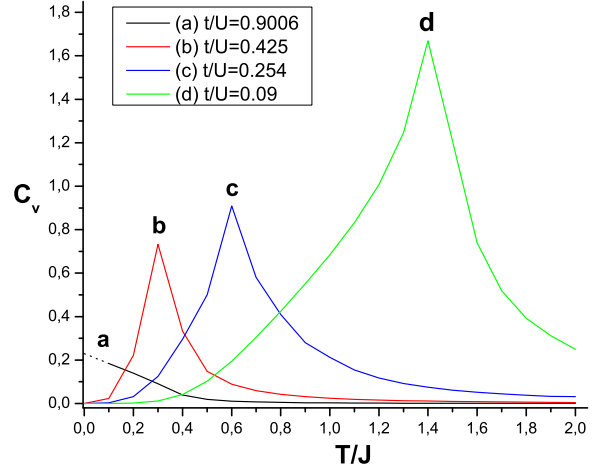


FIG. 6: (Color online) Contribution of magnons' fluctuations to the specific heat: (a) at quantum critical point $t/U = 0.9$ ($m_{cr} = 0.078$); (b) at $t/U = 0.425$ ($m = 0.175$); (c) at $t/U = 0.254$ ($m = 0.3$); (d) at $t/U = 0.09$ ($m = 0.5$).

very sharp peak at ambient pressure. With increasing pressure the magnetic anomaly remains well defined but maximum decreases. This phenomena is well described theoretically in the present paper Fig.(6). The existing correspondence between specific heat and derivative of the resistivity suggests a confidence that magnon's fluctuations are important and for the transport properties of the itinerant antiferromagnets.

VI. SUMMARY

In this paper an itinerant antiferromagnets were studied. Varying the ratio t/U , where t is the hopping parameter and U is the Coulomb repulsion, the system was investigated between a state with localized spins ($t/U < 0.09$) and quantum critical point $t/U = 0.9$ at which Néel temperature is zero. The evolution of the magnons' fluctuations in antiferromagnetic and paramagnetic phases was studied by means of the renormalized spin-wave theory and modified spin-wave theory. The renormalized spin-wave theory includes a parameter r which accounts for magnon-magnon interaction. The system of equations for the Néel temperature (42) rewritten for 2D system has the only solution $T_N = 0$. This shows that present method of calculation is in accordance with Mermin-Wagner theorem, which is our theoretical criteria for adequate account of magnons's fluctuations. The modified spin-wave theory involves in a natural way the gap of the magnon in paramagnetic phase.

The effective spin is the most important factor which determines the quantum criticality. To figure out this one has to map the low-energy excitations of the half-filled Hubbard model onto an effective spin-1/2 Heisen-

berg model [24]. The dimensionless Néel temperature T_N/J for this model is $T_N/J = 1.387$. The result shows that the Néel temperature of the spin-1/2 antiferromagnets is nonzero for all values of the exchange constant including weak coupling $U/t \ll 1$ regime [24]. This is in contrast to the result in the preset paper where the antiferromagnetism is destroyed at $U/t < 1.11$ ($t/U > 0.9$). The mapping of the Hubbard model onto an effective Heisenberg model with effective spin- $m < 1/2$ is a crucial step towards the understanding of quantum criticality.

The critical value of the effective spin $m = 0.078$ only depends on the effective Heisenberg model. The effective exchange constant J and the effective spin m are calculated in one fermion-loop approximation. It is neither strong coupling approximation nor weak coupling approximation. At half filling the chemical potential is fixed $\mu = U/2$ and the dispersions' Eq.(19) dependence on the parameter t/U is nontrivial.

To compare with experimental results the phase diagram in plane of T/U and control parameter t/U was obtained. To compare with results of the numerical calculations one has to convert the diagram Fig.(3) into phase diagram in plane of T/t and U/t . The result is shown in figure (7).

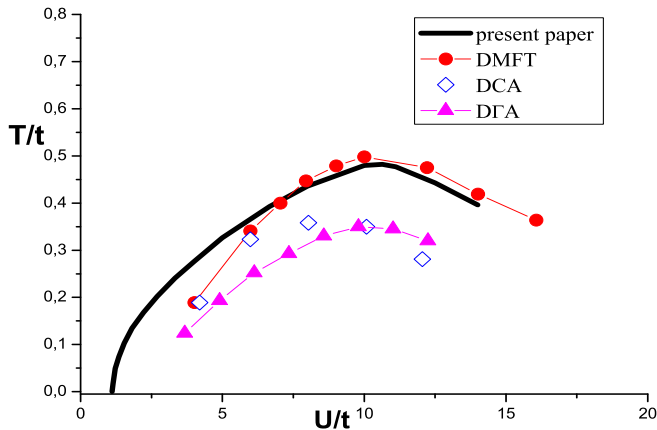


FIG. 7: (color online) Phase diagram in plane of temperature T_N/t and control parameter U/t . The solid black line is the phase diagram obtained in the present paper. The red circles, the blue open diamonds and the magenta triangles are the results in (DMFT), (DCA) and (DfA) respectively.

The solid black line is the phase diagram obtained in the present paper. The red circles, the blue open diamonds and the magenta triangles are the results obtained by means of the dynamical mean field theory (DMFT) [28], dynamical cluster approximation (DCA)[28] and dynamical vertex approximation (DfA) [30], respectively.

One of the most important point in the Hubbard model is the maximum of the Néel temperature T_N/t as a function of U/t . It indicates the crossover from itinerant magnetism to the magnetism of the localized spins. The Néel temperature of itinerant systems increases, when U/t increases, as a result of the increasing of the effective spin. The Néel temperature of the spin-1/2 Heisenberg model of localized electrons is $T_N = 1.387J$ with exchange constant which decreases when U/t increases. In the present paper the maximum is at $U/t = 10.6$, in the DMFT at $U/t = 10$ and in DfA at $U/t = 9.8$. The overall agreement of the results for the Néel temperature in the present paper with the results obtained in DMFT are satisfactory for all values of U/t except for lowest one. The non-local corrections, accounted for in DfA, reduce the Néel temperature T_N/t versus temperatures in DMFT and present paper in whole phase diagram.

The exchange constant J of the effective model Eq. (17) is calculated in the limit when the frequency and the wave vector are small. The calculations can be improved employing an effective Heisenberg theory with exchange constant $J(k)$ which depends on the wave vector k .

Another important point in the Hubbard model is the quantum critical point (QCP) $T_N = 0$. The phase diagram Fig.(7) shows that it is reached at $U/t = 1.11$. The figure also shows that all numerical calculations are implemented at control parameters $U/t > 3.674$, which is far from the QCP. This explains the absence of comments on the quantum criticality. On the other hand an investigation of the Hubbard model without explicit affirmation of existing or nonexisting of QCP in the Hubbard model is not complete. One can extrapolate the curves in DMFT, DCA and DfA down to zero temperature. A non-zero QCP emerges in these approaches.

Alternatively, the Hubbard model is studied by a mapping on a spin-1/2 generalized Heisenberg model with higher order terms in a form of long-range or ring exchange [41]. An effective Heisenberg model with spin-1/2 is considered which can not describe the quantum criticality despite the fact that parameter t/U is close to the quantum critical point. This is because the quantum critical behavior depends decisively on the effective spin of the itinerant electron which is smaller than 1/2 near the quantum critical point (see figure (2)).

Néel order and quantum critical point in the Hubbard model are also studied by means of a spin-charge rotating reference frame approach [42], which explicitly factorizes the charge and spin contribution to the electron operator. The effective constants are calculated by means of Hartree-Fock approximation of the fermion interaction. This explains the over estimation of the critical value of the control parameter $U/t = 0.676$ ($t/U = 1.479$) compare with the result in the present paper $t/U = 0.9$, where the Coulomb repulsion is treated exactly.

VII. ACKNOWLEDGMENTS

This work was partly supported by a Grant-in-Aid DO02-264/18.12.08 from NSF-Bulgaria. The author ac-

knowledges the financial support of the Sofia University.

-
- [1] F. M. Grosche, S. R. Julian, N. D. Mathur, and G. G. Lonzarich, *Physica B* **223-224**, 50 (1996).
 - [2] R. Movshovich, T. Craf, D. Mandrus, J. D. Thompson, J. L. Smith, and Z. Fisk, *Phys. Rev. B* **53**, 8241 (1996).
 - [3] N. D. Mathur, F. M. Grosche, S. R. Julian, I. R. Walker, D. M. Freye, R. K. W. Haselwimmer, and G. G. Lonzarich, *Nature* **394** 39 (1998).
 - [4] F. M. Grosche, I. R. Walker, S. R. Julian, N. D. Mathur, D. M. Freye, M. J. Steiner, and G. G. Lonzarich, *J. Phys. Condens. Matter* **13**, 2845 (2001).
 - [5] S. Araki, M. Nakashima, R. Settai, T. C. Kobayashi, and Y. Ōnuki, *J. Phys.: Condens. Matter* **14**, L377 (2002).
 - [6] M. Yashima, S. Kawasaki, H. Mukuda, Y. Kitaoka, H. Shishido, R. Settai and Y. Onuki, *Phys. Rev. B* **76** 020509 (2007).
 - [7] T. Moriya, *Spin Fluctuations in Itinerant Electron Magnetism* (New York: Springer 1985).
 - [8] S. Sachdev, *Quantum Phase Transition* (Cambridge University Press, Cambridge 1999).
 - [9] G. G. Lonzarich, in *Electron* ed M. Springford (Cambridge University Press, Cambridge 1997).
 - [10] S. A. Grigera, R. S. Perry, A. J. Schofield, M. Chiao, S. R. Julian, G. G. Lonzarich, S. I. Ikeda, Y. Maeno, A. J. Millis, A. P. Mackenzie, *Science* **294**, 329 (2001).
 - [11] Matthias Vojta, *Rep. Prog. Phys.*, **66** 2069 (2003).
 - [12] Hilbert v. Löhneysen, Achim Rosch and Matthias Vojta, and Peter Wölfle, *Rev. Mod. Phys.*, **79**, 3 (2007).
 - [13] Christian Pfleiderer, *Rev. Mod. Phys.*, **81** 1551 (2009).
 - [14] Qimiao Si and Frank Steglich, *Science* **329** 1161 (2010).
 - [15] Georg Knebel, Dai Aoki, and Jacques Flouquet, *arXiv:1105.3989* (2011).
 - [16] J. E. Hirsch, *Phys. Rev. B* **35**, 1851 (1987).
 - [17] R. T. Scalettar, D. J. Scalapino, R. L. Sugar, D. Tous-saint, *Phys. Rev. B* **39**, 4711 (1989).
 - [18] M. Ulmke, R. T. Scalettar, A. Nazarenko and E. Dagotto, *Phys. Rev. B* **54**, 16523 (1996).
 - [19] R. Staudt, M. Dzierzawa, and A. Muramatsu, *Eur. Phys. J.*, **B 17**, 411 (2000).
 - [20] Y. Kakehashi, P. Fulde, *Phys. Rev. B* **32**, 1595 (1985).
 - [21] Y. Kakehashi, J.H. Samson, *Phys. Rev. B* **33**, 298 (1986).
 - [22] P. G. J. van Dongen, *Phys. Rev. Lett.* **67**, 757 (1991).
 - [23] P. G. J. van Dongen, *Phys. Rev. B* **50**, 14016 (1994).
 - [24] Y. H. Szczech, M. A. Tusch, D.E. Logan, *Phys. Rev. Lett.* **74**, 2804 (1995).
 - [25] M. Jarrell, *Phys. Rev. Lett.* **69**, 168 (1992).
 - [26] A. Georges, W. Krauth, *Phys. Rev. B* **48**, 7167 (1993).
 - [27] M. Ulmke, V. Janis, D. Vollhardt, *Phys. Rev. B* **51**, 10411 (1995).
 - [28] P. R. C. Kent, M. Jarrell, T. A. Maier, and Th. Pruschke, *Phys. Rev. B* **72**, 060411 (2005).
 - [29] Sebastian Fuchs, Emanuel Gull, Lode Pollet, Evgeni Borovski, Evgeni Kozik, Tomas Prushke, and Mattias Troyer, *Phys. Rev. Lett.* **106**, 030401 (2011).
 - [30] A. Toschi, A. A. Katanin, and K. Held, *Phys. Rev. B* **75**, 045118 (2007).
 - [31] G. Rohringer, A. Toschi, A. A. Katanin, and K. Held, *Phys. Rev. Lett.* **107**, 256402 (2011).
 - [32] G. Knebel M-A Méasson, B. Salce, D. Aoki, D. Braithwaite, J. P. Brison, and J. Flouquet, *J. Phys.: Condens. Matter* **16**, 8905 (2004).
 - [33] N. D. Mermin and H. Wagner, *Phys. Rev. Lett.* **17**, 1133 (1966).
 - [34] D. Schmeltzer, *Phys. Rev. B* **43**, 8650 (1991).
 - [35] The vertexes of the Brillouin zon are topologically equivalent. This is why we have two long-range excitations in the theory.
 - [36] M. Takahashi, *Prog. Theor. Physics Supplement* **87**, 233 (1986).
 - [37] M. Takahashi, *Phys. Rev. Lett.* **58**, 168 (1987).
 - [38] M. Takahashi, *Phys. Rev. B* **40**, 2494 (1989).
 - [39] J. E. Hirsch and Sanyee Tang, *Phys. Rev. B* **40**, 4769 (1989).
 - [40] H. Hegger, C. Petrovic, E. G. Moshopoulou, M. F. Hundley, J. L. Sarrao, Z. Fisk, and J. D. Thompson, *Phys. Rev. Lett.*, **84**, 4986 (2000).
 - [41] Alexander Reischl, Ervin Müller-Hartmann, and Götz S. Uhrig, *Phys. Rev. B* **70**, 245124 (2004).
 - [42] T. A. Zaleski and T. K. Kopeć, *Phys. Rev. B* **77**, 125120 (2008).